

# The Physics of MRI- Basic Spin Gymnastics

D.B. Plewes, PhD, W. Kucharczyk, MD  
Departments of Medical Biophysics and Medical Imaging  
University of Toronto  
Oct 2003 (Revised webpage)

## Introduction

To understand MRI, it is first necessary to understand the physics of proton Nuclear Magnetic Resonance (NMR). The most important site of this resonance relevant to MRI is the nucleus of the hydrogen atom in water. While other protons occurs within biological molecules, water represents the most important site for MRI due to the concentration of protons in water and the dynamical properties of water.

The proton is a fundamental nuclear particle which exhibits charge, mass and spin (FIGURE 1). While the first of these two concepts is familiar, the notion of spin is not as well appreciated. As the name suggests, it can be thought of as a rotation of the nucleus about its axis which in conjunction with the charge of the nucleus, gives the proton a magnetic property similar to a small bar magnet. However, in addition to the magnetic property of the nucleus, the spin together with the mass of the proton, gives it a property referred to as angular momentum. The combined effect of the spin, charge and mass are the three ingredients, which are responsible for NMR.

Specifically, when a proton is placed in an applied magnetic field, it will precess or wobble. This precession is similar to that of a spinning gyroscope when placed in the earth's gravitational field. In this case, the gyroscope appears to wobble about its axis at a specific frequency dictated by the strength of the gravitation field and the rotation characteristics of the gyroscope. In a similar manner, the proton's precessional frequency, also known as the Larmor frequency, is dictated by the fundamental properties of the proton and is proportional to the strength of the magnetic field. For example, at a field strength of 1 Tesla (approximately 30,000 times stronger than the earth's magnetic field), the Larmor frequency is 42.57 Mhz. Doubling the magnetic field strength to 2 Tesla would increase the Larmor frequency to 85.14 MHz.

The scaling factor between Larmor frequency and magnetic field is known as the gyromagnetic ratio  $\gamma$  and is tabulated in (FIGURE 2) along with the relative sensitivity of the NMR signal for various nuclei of biological interest. It is noteworthy, that not all nuclei can generate an NMR signal. Only isotopes with an odd number of protons or neutrons have a non-zero spin which permits the formation of an NMR signal. This figure shows that the nucleus of hydrogen, gives the biggest signal largely due to its gyromagnetic ratio and the fact that the most abundant isotope of hydrogen exhibits a spin. In comparison, the relevant isotopes of carbon, sodium or phosphorous are less abundant and therefore generate a much weaker NMR signal.

## Detecting and Exciting NMR

As indicated above, a proton has a specific resonance frequency for a fixed magnetic field. We can represent the collective magnetic properties of the protons as a vector (FIGURE 3) corresponding to the "bulk magnetization" which precesses about the magnetic field  $B_0$  at a frequency given by  $\gamma B_0$ . In order to detect this magnetization, we use a coil of wire which is connected to a sensitive amplifier (FIGURE 3) which is in turn tuned to the Larmor frequency. The rotating magnetic field from the magnetization will induce a tiny NMR signal in the coil, which oscillates at the Larmor frequency. Only the time varying part of the magnetization is capable of

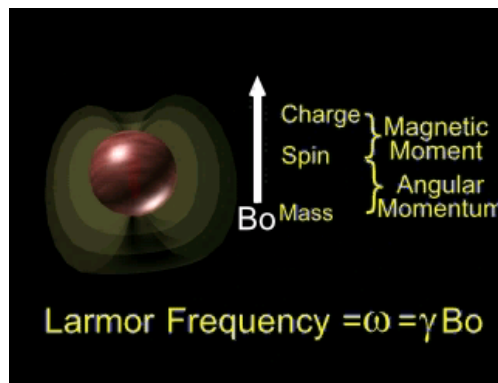


**Figure 1.** The precession of a proton in a magnetic field  $B_0$ , arises from its charge, mass and spin.

NMR Parameters of Common Elements			
Nucleus	Spin	Gyromagnetic ratio	Relative Sensitivity
$^1\text{H}$	1/2	42.57	1.00
$^{13}\text{C}$	1/2	10.70	0.015
$^{19}\text{F}$	1/2	40.05	0.833
$^{31}\text{P}$	1/2	17.235	0.066
$^{23}\text{Na}$	3/2	11.262	0.092

**Figure 2.** NMR parameters for key biological elements

inducing a signal in the coil and as such only the rotating component of the magnetization in the x-y plane (FIGURE 3) is detectable by this method. This component of the magnetization is referred to as the “transverse” component as opposed to the “longitudinal” component parallel to the  $B_0$  field. This also means that the orientation of the receiver coil must be such that its axis lies in the transverse plane (FIGURE 3), so that the changing magnetic field of the transverse component can couple with the coil and induce a signal.

Normally, the magnetization is aligned parallel to the  $B_0$  field (along the z axis) and as such cannot precess. In order to generate an NMR signal, we must tip the magnetization away from this equilibrium alignment so that a component of the magnetization lies in the transverse plane where it is free to precess. To achieve this, the spins are exposed to an alternating “ $B_1$ ” magnetic field (FIGURE 4) which is tuned to the Larmor frequency. As the Larmor frequencies are typically in the Mhz range, these pulses are referred to as radio frequency or “RF” pulses. Unlike the  $B_0$  field, the direction of the  $B_1$  field is in the transverse plane. By virtue of this alternating applied magnetic field, the spins can progressively absorb energy and by tipped away from the longitudinal axis to create a component into the transverse plane. The longer the duration of the applied field, or the greater its field strength the greater the tip angle which can be achieved. By careful choice of the duration and strength of this applied  $B_1$  field, the magnetization can be tipped to any angle relative to the Z-axis.

### The Rotating Frame of Reference

The motions of the magnetization vector are complex as they rotate out of alignment with the Z-axis and precess about the Z-axis during excitation and relaxation. In order to simplify our picture of these motions, it is common to view the spin system from a special frame of

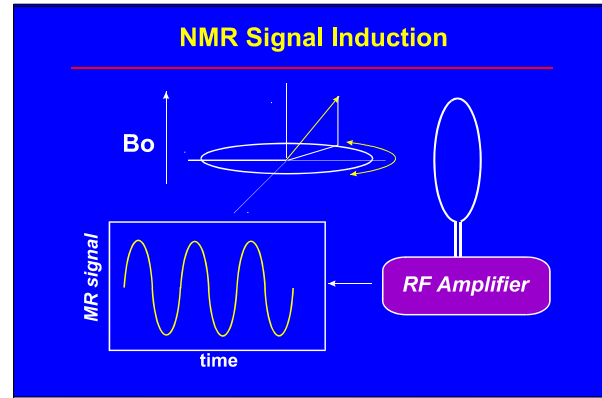


**Figure 3.** The induction of the NMR signal in a tuned receiver circuit.

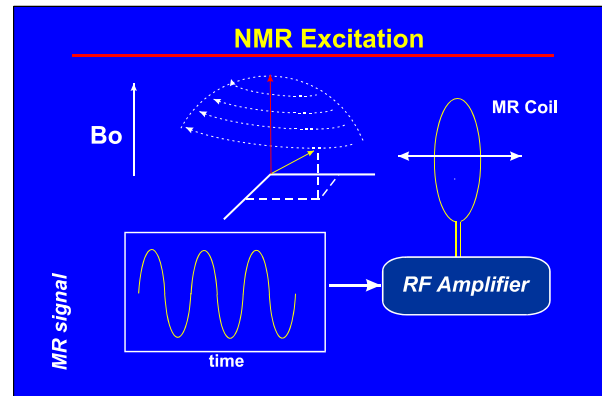


**Figure 4.** The excitation of NMR by the application of an RF pulse at the spin Larmor frequency.

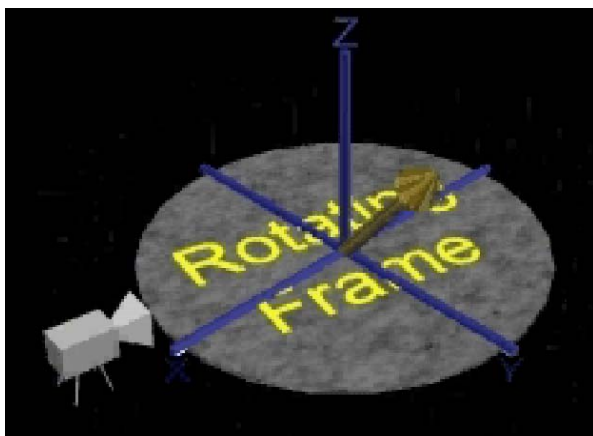


**Figure 5.** Viewed from the rotating frame, the precessing spin appears motionless.

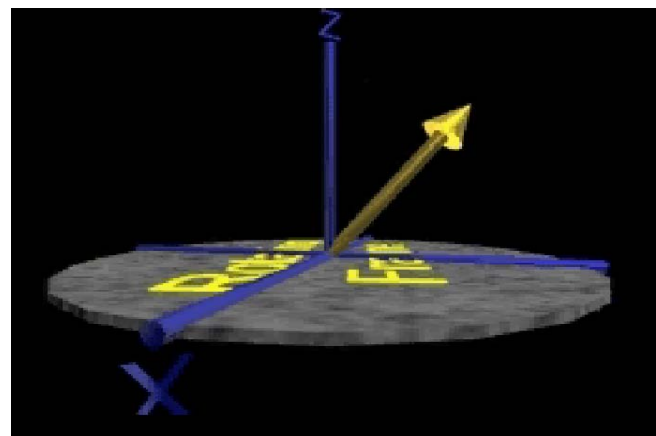


**Figure 6.** A precessing spin precessing while a camera is mounted on a turntable which rotates at the same Larmor frequency.

reference which itself rotates about the Z-axis (FIGURES 5 & 6). To appreciate this concept, imagine a turntable that revolves about the Z-axis at the Larmor frequency carrying a small camera (FIGURE 5). As viewed from the “Laboratory” frame, we see the magnetization,

turntable and the camera rotating about the Z-axis in synchrony. However, if we view the magnetization vector from the point of the view of the rotating camera, we would see that the magnetization vector would appear stationary with a fixed alignment relative to the Z without any precession (FIGURE 6). From this new point of view, we see that the precessional motion of the spins can be simplified. Furthermore, if the spin precesses at a frequency which is slightly slower or faster than the frequency of the rotating frame of reference, the spin will precess in this frame at a frequency which corresponds to the difference between the spin precession frequency and that of the rotating frame. Thus, the spin can appear to precess in either direction with its frequency dictated by this difference frequency.

### Spin Dephasing and Transverse Signal Decay

In order to appreciate the contrast mechanisms in MRI, it is necessary to understand how the magnetization of the multitude of spins in the object combines to produce the NMR signal. Recall, that vectors which are parallel or “in-phase” (FIGURE 7), add in proportion to their individual lengths. However, if the vectors are not aligned, or are slightly “out-of-phase”, their sum will reflect both their magnitudes and orientations as shown in FIGURE 7. Thus if we consider spins with identical frequencies which are matched to the rotating frame, the magnetization of each spin will add in phase and thus be the numeric sum of their individual magnetization. However, if we consider a situation in which each spin experiences a slightly different magnetic field, then each will have a slightly different precession frequency (FIGURE 8). Assuming that the spins are initially aligned, this difference in frequency will cause the phase angle of each component of the magnetization to progressively drift out of alignment. Thus with increasing time, the sum of the individual magnetization vectors will decrease due to this progressive de-phasing resulting in a decay of the NMR signal (FIGURE 8). The time constant for this signal decay can be characterized as that time needed to reduce the signal to  $1/e$  or 37% of its maximum value and is referred to as  $T2^*$ .

At this point, it would be natural to ask what mechanisms cause the spins to experience different magnetic fields throughout the tissue. First, we should categorize these field variations into two groups; those which are fixed in time as distinct from those which change with time. Fixed inhomogeneities of the magnetic field could result from the design of the magnet used to form the  $B_0$  field and as such are uninteresting from a biological point of view. However, even with a perfect magnet, the tissues being imaged can distort the fields as a result of their magnetic properties. Changes in tissue magnetic “susceptibility” can generate small field gradients on the order of a few parts per million that can vary throughout the tissue. As these inhomogeneities are fixed, the phase angle of individual spins will grow at a constant rate.

In contrast to fixed field variations, there are other mechanisms that can generate time varying field inhomogeneities. These can arise from the fact that the protons themselves are slightly magnetic which can exchange magnetization or due to diffusive movement of spins in microscopic magnetic field inhomogeneities. This decay mechanism is referred to as spin-spin relaxation and has a decay time or  $T2$  (FIGURE 9). The key point is that spin-spin relaxation arises from these time varying magnetic spin

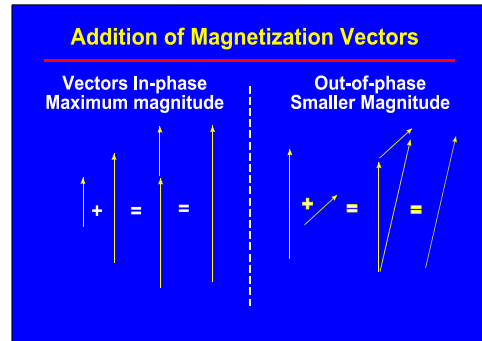


**Figure 7.** Addition of vectors taking into account their orientation or phase.

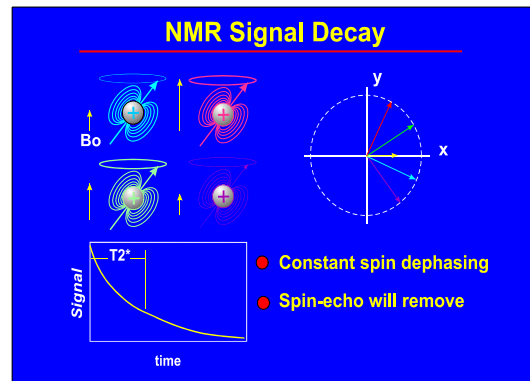


**Figure 8.** Signal loss due to spins losing phase coherence.

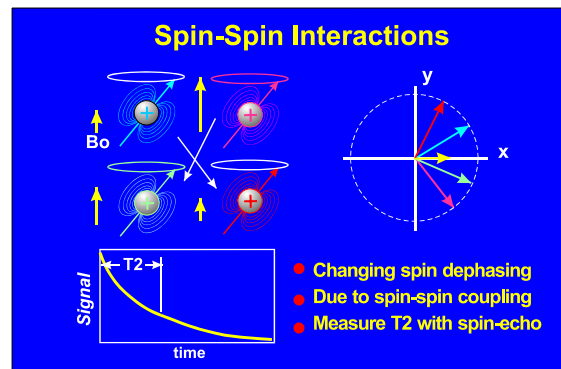


**Figure 9.** Spin-Spin relaxation arising from random motion of spins in magnetic field gradients and spin-spin interactions.

interactions. As such, the rate of spin dephasing arising from spin-spin interactions is not constant. In any NMR experiment, spins will experience spin dephasing from both fixed and time varying field changes and both of these factors contribute to the decay time constant  $T2^*$ . However, using a special combination of excitation pulses, known as a spin-echo pulse sequence, it is possible to measure the signal decay time constant arising only from the time varying changes in the magnetic field to quantify  $T2$ .

### Spin-Spin Relaxation and T2 Weighted MRI

The spin-echo pulse sequence uses two RF pulses as shown in FIGURE 10. The first pulse tips the spins by  $90^\circ$  to force the total magnetization onto the transverse plane. Immediately after this pulse, the spins are in-phase and the NMR signal is maximized. Shortly thereafter, the spins undergo dephasing and the signal decays. At some arbitrary time ( $TE/2$ ) after the first RF pulse, a second RF pulse is delivered which rotates all the spins by an additional  $180^\circ$  as shown in FIGURE 10. This moves the spins into an arrangement which mirrors their positions just prior to the  $180^\circ$  pulse. At a later time  $TE$  seconds after the  $90^\circ$  RF pulse, we find that the signal reappears to form an 'echo'. The reason for this 'spin-echo' can be understood by considering the phase of a single spin. During the first  $TE/2$  seconds, a spin will accumulate a phase angle of  $\theta$  degrees (relative to the positive Y axis). After the second RF pulse, the phase of this same spin is now  $180-\theta$  degrees. This indicates that the phase of the spin is exactly  $\theta$  degrees from the negative Y-axis. Thus, assuming that the spin continues to accumulate phase at the same rate, the phase will align with the negative Y-axis in an additional  $TE/2$  seconds after the  $180^\circ$  pulse, or  $TE$  seconds after the original  $90^\circ$  RF pulse. This argument holds true for all the spins in the system, so that all the spins will re-align along the negative Y-axis to form a spin-echo at a time  $TE$ .

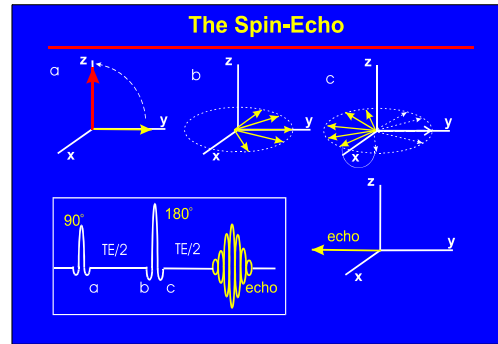


**Figure 10.** The Spin-Echo experiment which is the foundation for the measurement for spin-spin or  $T2$  relaxation times.

If the rate of dephasing for all spins were constant during the  $TE$  interval, the magnitude of the transverse magnetization at  $TE$  would be identical to the magnetization immediately after the first  $90^\circ$  RF pulse. However, the time varying nature of spin dephasing outlined above, will create small variations in the phase angle accumulation for each spin before and after the  $180$  degree RF pulse. The net result is that the spins will not perfectly align at time  $TE$  resulting in a small net spin dephasing and signal decay. The longer the  $TE$  interval, the greater the opportunity for spin dephasing resulting in a greater signal loss.

A plot of echo amplitude for varying  $TE$  will show a signal decay with a time constant  $T2$  (FIGURE 9). By this experiment, it should be clear, that only the signal loss associated with the time varying component of spin dephasing will contribute to the echo amplitude and thus allows us to measure  $T2$  independently of static field inhomogeneities. As a result,  $T2$  will always be longer than  $T2^*$  as the latter time constant suffers from both static and time varying dephasing while  $T2$  only experiences time varying dephasing.

The consequence of  $T2$  relaxation on MRI is very briefly summarized in FIGURE 11. In the case of a spin-echo MR pulse sequence, the  $90^\circ$  and  $180^\circ$  pulses are used to form the spin-echo from which the MR image is formed and it is the magnitude of this echo which determines the brightness in the MR image. If we have two tissues of differing  $T2$  values, the echo amplitudes for each tissue at time  $TE$  will differ depending on their respective  $T2$  values. Typical  $T2$  times for tissues in the brain are summarized in FIGURE 12. Thus in a

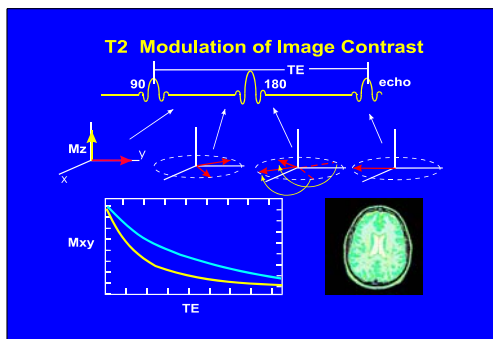


**Figure 11.** The effect of spin-spin relaxation on the brightness of tissues in a spin-echo MR image.

$T2$  weighted MR image, CSF will be brighter than either grey or white matter, consistent with the tabulated values of FIGURE 12.

## The Spin-Lattice Relaxation Time and T1 Weighted Imaging

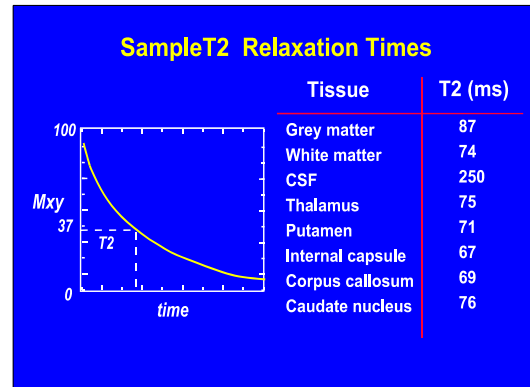
In the preceding section, we reviewed how spins dephase and cause a loss of detected signal. However, it is important to note that spin dephasing is a loss of the arrangement of spin orientation after the initial excitation pulse. In this case, the energy which has been deposited by the RF excitation pulse has not been dissipated but only lost to detection. However, if we wait longer, this energy will slowly leave the spin system and be distributed throughout the sample or the “lattice”. The time required for this dissipation is referred to as the spin-lattice or T1 time constant and tend to be longer than the T2 time constant of a given tissue. As a result, after the spins have undergone signal loss from dephasing, the magnetization slowly grows along the z-axis until the equilibrium magnetization is finally reached (FIGURE 13). The time needed to reach 63% of the equilibrium longitudinal magnetization is referred to as the T1 time constant. T1 values for biological tissues generally increase with Larmor frequency whereas T2 times are relatively constant. Typical values for the head are shown in FIGURE 13 for a field strength of 1.5 Tesla. Comparing values from FIGURES 12 and 13 is clear that T1 tend to be 5 to 10 times longer than T2 for these tissues at 1.5 Tesla.

Images reflecting T1 are commonly made in MRI and the details of image contrast are complex and beyond to scope of this lecture. However, a very simple presentation is illustrated in FIGURE 14. As we will see, spin-echo MR images are made with multiple repetitions of a  $90^\circ$  and  $180^\circ$  pulse combination followed by the detected spin-echo. This triplet of pulses is repeated multiple times every TR seconds in order to gather enough data for form an MR image. Thus it can be seen that the extent of recovery of equilibrium magnetization during the TR interval will vary depending on the tissue T1 value. A tissue with a longer T1 will recover less and contribute less to the spin-echo relative to a tissue with a shorter T1 relaxation time. As such, the short T1 tissue will appear brighter than the longer T1 tissue. While we have made this point in the context of spin-echo MRI, it is true for all MRI techniques requiring multiple excitations to collect MRI data.

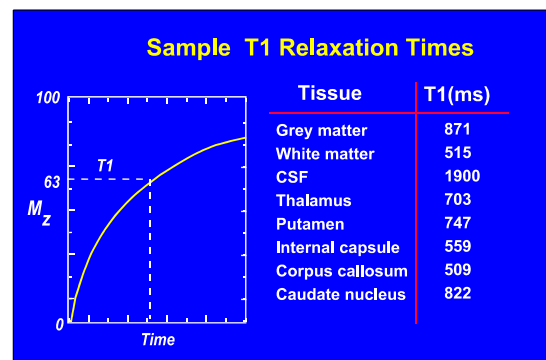
### Summary of Relaxation Mechanisms for Proton MRI

We have seen that there are two main relaxation mechanisms of interest in proton MRI; namely, spin-lattice (T1) and spin-spin(T2) relaxation. Spin-spin relaxation is an example of a relaxation mechanism which is associated with a loss of spin order or phase and is seen as a transverse decay of signal after the initial spin excitation. The spin-spin time constant T2 is measured with a spin-echo experiment. A related time constant T2\* is also seen as a signal decay from spin dephasing and is the time constant observed by simply observing the signal decay directly. In this case T2\* is shorter than T2 as it includes dephasing mechanisms from both constant and time varying magnetic field inhomogeneities throughout the tissue.

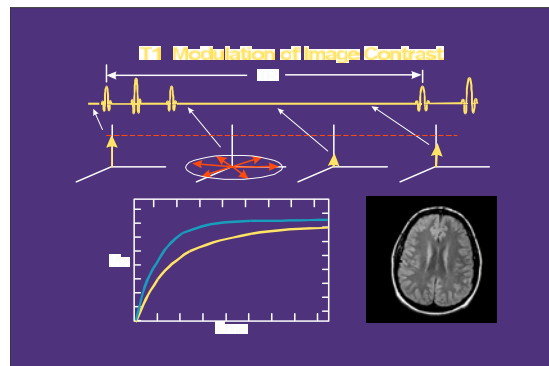
In contrast, T1 is the time needed for the spin system to dissipate the energy which was deposited in the tissue by the initial RF excitation pulse. In liquids, this energy dissipation is slow by comparison to the time to cause the spin system to dephase, thus T1 times are much longer than either T2 or T2\*. From this discussion, it is clear that T2 can never be larger than T1.



**Figure 12.** Table of T2 relaxation times for various tissues.



**Figure 13.** T1 or Spin-Lattice relaxation times at 1.5 Tesla for various tissues.



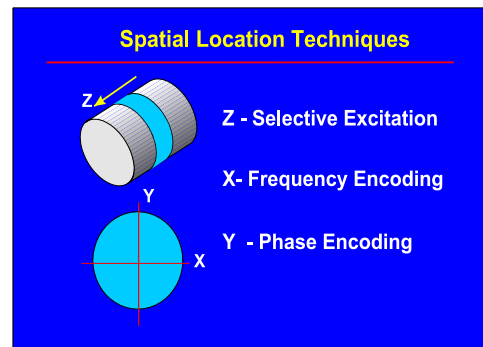
**Figure 14.** T1 modulation in spin-echo MRI.

Image contrast arising from either T2 or T1 relaxation mechanism is complex and is modulated by the timing of pulses sequences and size of the flip angles resulting from the excitation pulses. Changing the TE times of spin-echo experiments will alter the T2 weighting while altering the TR interval or flip angle will control the T1 weighting in MR images.

In the preceding sections, we discussed the very basic physics of how NMR signals are generated and the time constants dictating the nature of the evolution of the transverse and longitudinal magnetization. In the following sections, we will describe how, the unique physics of NMR can be used to create beautiful images of the anatomy.

### Image Formation Based on NMR

MRI is unique as a medical imaging method in terms of the relation between the detected signals and the final image. As in any digital imaging method, the challenge of MRI is to define the intensity of the MRI signal for an array of pixels corresponding to differing points throughout the anatomy. However, unlike all other imaging methods in current use in medical imaging, the signal detecting device (receiver coils) cannot be collimated to restrict the signal to a specific location as is done in x-ray imaging, ultrasound or radionuclide imaging. Rather, the MR imaging task is unique, as the detected signals originate from the entire object rather than a single point within it. Thus in the following sections, we illustrate the mechanisms used to achieve a MR images based on the fact that spins precess at a frequency proportional to the surrounding magnetic field. We will do this by recognizing that our goal is to find the brightness of pixels located in a three dimensional co-ordinate system based (X,Y and Z) and use three related techniques to achieve this based on selective excitation, frequency and phase encoding (FIGURE 15). To achieve this we will deliberately distort the magnetic field in the magnet to provide spatial encoding through the use of magnetic field gradients. In the next section, we will describe the meaning of these gradients which will become critical to our understanding of MRI.



**Figure 15.** The spatial localization task and the MRI methods used to achieve them.

### Magnetic Field Gradients

Great care is used to build the magnets for MRI so as to achieve a highly homogeneous magnetic field within the magnet bore. However, in order to create MR images, these fields must be distorted in a precise and controlled manner through the applications of magnetic field gradients. To illustrate this more fully consider the object in the presence of a gradient in the X direction as shown in FIGURE 16. A gradient in the X direction means that the field changes only in the X direction and is constant for any point in a Z-Y plane. Furthermore, the field on this plane either increases/decreases with the +ve X position and decreases/increases with the -ve X location. Similarly, a gradient in Z means that the field is proportional only the Z location and is constant in a X-Y plane. Finally, the Y gradient causes the field to change only in the Y direction and is constant within a Z-X plane. In addition, to these gradients having a direction such as X, Y or Z, they can also have a magnitude. In this case, the meaning of the magnitude of the gradient refers to the rate with which the field changes per unit distance. Typical gradients can have values of 10 mT/m, meaning that the field changed 10 mT (i.e.  $10^{-2}$  Tesla) for every meter of distance moved in object. Thus in comparison to the size of the applied magnetic field ( $\sim 1$  Tesla), we see that these gradients represent very small perturbations ( $\sim 1\%$ ) to the overall field. As these gradients have both magnitude and direction they can be represented as vectors and can add to generate gradients in any direction by the simultaneous application of component X, Y and Z gradients.

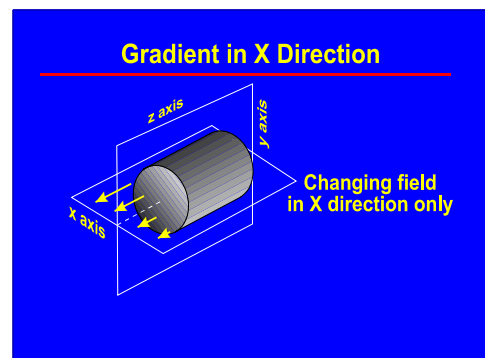


**Figure 16.** An illustration of the concept of a magnetic field gradient in the x-direction.

## Selective Excitation

The task of defining the 3D distribution of image brightness generally starts with “selective excitation”. As the name implies, this process creates a slab of tissue which is excited so that transverse magnetization is restricted to a specific plane of prescribed location and thickness. The technique involves the combination of NMR resonance, magnetic field gradients and a band limited RF excitation pulse. An analogy to selective excitation is illustrated in

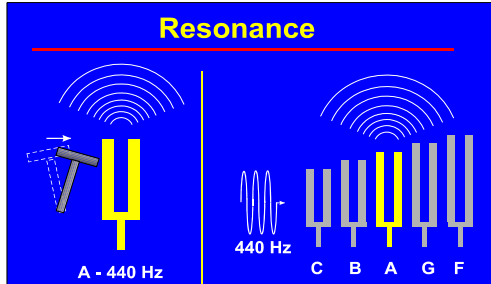


**Figure 17.** An array of tuning forks which are undergoing selective excitation by an acoustic source tuned to the note A=400 Hz.

arranged in a linear array from F to C and since we used A to excite the array, we know that the middle tuning fork must have undergone excitation. By this means, we can excite a specific location in space by the choice of the excitation tuning fork. It follows that using an excitation tuning fork of higher or lower frequency will move the excited region to right or left.

This simple analogy is perfectly adaptable to NMR selective excitation. In this case, the spins can absorb energy only if the RF frequency is matched to the Larmor frequency. To create an arrangement similar to the line of tuning forks, we use a magnetic field gradient as discussed above. In this situation, the magnetic field changes along the axis of the object as shown in FIGURE 18. In this case, the near end of the cylinder experiences a smaller field and lower Larmor frequency than the opposite end. Thus, we can consider the object to be composed of different slabs of varying Larmor frequency. Applying the RF excitation to match a frequency for the centre slab will rotate magnetization in this slab to the transverse plane where it will continue to precess. By controlling the range of frequencies used in the excitation pulse, we can control the width of the slice while controlling the centre frequency of the pulse, we can control the location of the slice. By this means, we have now created precessing magnetization in a slab of a specific location and slice thickness. The task which remains, is to define the brightness of the spins within this slab.

## Fourier Magnetic Resonance Imaging

In order to explain the basics of how the in-plane localization task is performed, we will proceed in a two-step manner as illustrated in FIGURE 19. First, we will show how MR images can be constructed from so-called K-space data. Once an intuitive understanding of the nature of K-space has been established, we will then indicate how the MR imaging system generates the image signals in the form of the required K-space data.

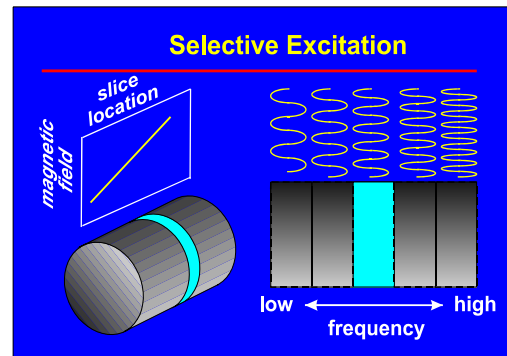


**Figure 18.** A magnetic field gradient in Z is used to create a range of Larmor frequencies which allow selective excitation of a specific

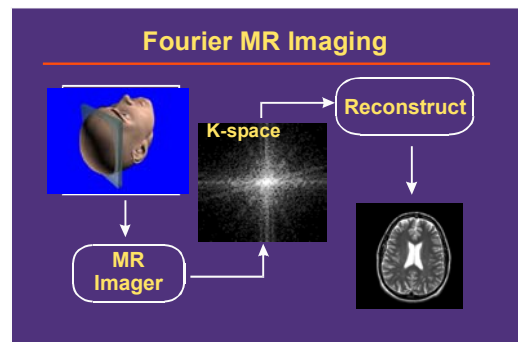


**Figure 19.** Fourier MRI involves the generation of data in K-space and the reconstruction of this data for form the final MR

## Image Space and K-Space

To start our understanding of how MR images are formed, we need to understand the relation between the MR image and its “K-space” representation. As shown in FIGURE 20, we see that the image has coordinates X and Y while the K-space data has coordinates  $K_x$  and  $K_y$ . The units of X and Y are in units of distance (i.e. centimeters) while the units of  $K_x$  and  $K_y$  are in units of 1/distance (i.e. centimeters<sup>-1</sup>). Thus we see that the K-space dimensions are somewhat unfamiliar as they are expressed in reciprocal distances. The gray scale of the K-space data reflects the value of the data at positions  $K_x$  and  $K_y$ .

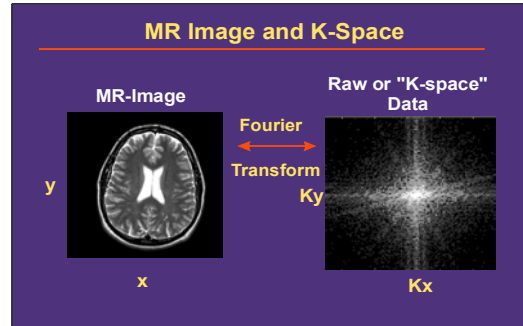


**Figure 20.** The relation between image space and K-space.

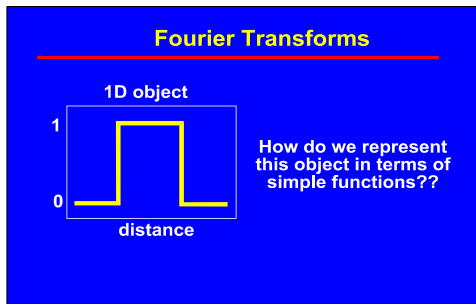


**Figure 21.** A one dimensional object to study K-space and Fourier synthesis.

distance which are the units of our K-space coordinates. When we add the constant and these two sine curves, we see that result oscillates over the right range and begins to approximate our target function (shown dotted in FIGURE 22). Rather than drawing tedious sine functions over the ROI, let us simplify our representation by plotting a graph (FIGURE 23) where we plot the amplitude of the sine functions versus their spatial frequency. This is a short hand graphical notation for the family of sine functions which, when added approximate the target function. The horizontal axis has units of spatial frequency (cycles/distance) while the vertical axis has units of amplitude. This is the K-space representation of our target function which is composed of three sine functions of frequency 0, 1 and 3 cycles/ROI. We can add more sine

In order to understand the meaning of the K-space representation, let us consider the simple problem of attempting to construct a mathematical formulae for the one-dimensional object or target function shown in FIGURE 21. The function is unusual, as it switches discontinuously from 0 to 1 over the region of interest (ROI). In order to appreciate how this can be done, we first consider the average value of this function which devotes 50% of its range to have a value of 0 with the remaining 50% with a value of 1, to give an average value of 0.5. So our first approximation of the target function is a constant of 0.5. Next we will add two sinusoidal function of varying amplitude and frequencies of 1 cycle and 3 cycles over the ROI. Thus these sine functions have an oscillation density or “spatial frequency” of a certain number of cycles per ROI. We can see that these frequencies have units of cycles per unit

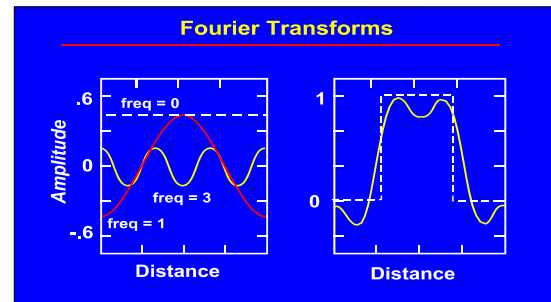


**Figure 22.** Using a constant and sinusoidal functions (left) to create an approximate version (right-yellow) of the target function (right-dotted).

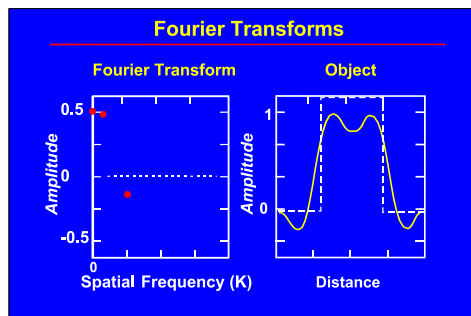


**Figure 23.** The K-space representation (left) of the Fourier components to create the target function (right).

functions (FIGURE 24) until we become arbitrarily close to the desired target function. The K-space representation and image domains are related through a mathematical operation called a Fourier transform. While the details of how this transform operates is beyond the scope of this lecture, the essential point is that it calculates the amplitudes and frequencies of sine curves chosen such that when they are all added together, we get the desired target function.

In order to represent a two dimensional function, such as a head image, one needs to use sine functions to exist in two directions. This is shown in FIGURE 25, where we show the K-space representation of the head image of FIGURE 20. Again, the relation between the K-space data and the image data are through a Fourier Transform. The brightness of a single point in

the K-space domain, reports the amplitude of the sine function, while the location of the point tells us its frequency and orientation. If we consider varying points (FIGURE 25) we can see that sine patterns of varying frequency and orientation are represented. To simplify our language, let us refer to these patterns of variously oriented sine functions as “stripes”. The intersection of the dotted lines represent the points of  $K_x=K_y=0$ . For point on the  $K_x$  axis the strips are vertical. For points on the  $K_y$  axis the strips are horizontal. For points with arbitrary  $K_x$  and  $K_y$  coordinates the strips are oblique. The angle of the stripe pattern is such that the strip density in x and y corresponds to the spatial frequency of the  $K_x$  and  $K_y$  component of the point in K-space. Remarkably, by combining all the points in K-space with their corresponding stripe amplitudes and frequencies, we generate the head image shown in FIGURE 20.

In summary, we see that the K-space representation is simply a short hand graphical notation which tells us the family of stripe functions, such that when they are added together, provide the desired image. The relation between the K-space representation of the image and the image is through a 2 dimensional Fourier transform. If we need to create an image with  $256 \times 256 = 2^{16}$  pixels in the image domain, the number of points in the K-space domain needed to characterize this image must also be  $2^{16}$  points.

### How the MR Imager Encodes Spatial Information

In the preceding section, we discussed the relation between the K-space domain and the image domain. In the remaining section, we discuss how the MR imaging system generates data directly in the K-space domain. We now recognize that the K-space domain, represents the image data as stripe functions of varying orientation, spatial frequency and amplitude. The question we address in this section, is how the MR imaging system generates these stripe functions and how it determines their correct amplitude, so that when added together, form the final image.

### Motions of Spins in a Gradient

Before we proceed further, it is helpful to change our representation of the magnetization that we discussed in the preceding sections from a vector to something simpler. Specifically, rather than drawing a rotating vector which induces a signal in the coil, let us represent the magnetization by a sphere. The sphere will rotate on its axis with one side of the sphere colored black, while the other side is white as shown in FIGURE 26. As the

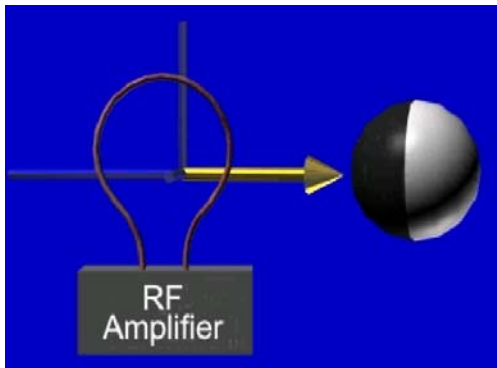


**Figure 26.** Using a rotating bi-colored sphere to represent the rotating transverse

magnetization rotates, the sphere revolves about its axis showing a progressive change from the white side to the black side. By looking at the progression of the color of the sphere, we can see the progression of the phase of the spin as it evolves in varying magnetic environments.

For our first example, let us consider a square array of balls as shown in FIGURE 27. After the excitation is created, the magnetization of each spin is in phase, and as such, all the balls are in the same orientation, showing the white face of each ball. Next we will consider the application of a gradient in the x-direction as shown by the graph of the gradient (right side of FIGURE 28) and the resulting magnetic field deviation shown at the bottom of this figure. When the gradient is applied, the balls experience slightly different magnetic fields. On the extreme left side, the magnetic field deviation is negative and causes the balls to rotate in a clockwise manner in the rotation frame. As we

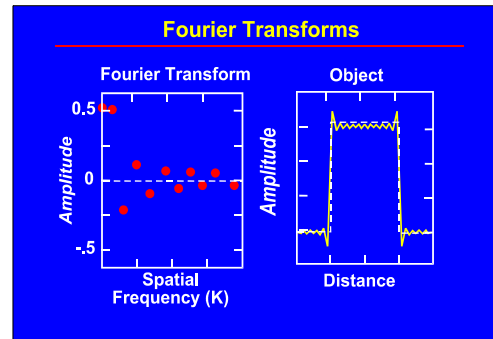


**Figure 24.** The K-space representation (left) of the Fourier components to create the target function (right).

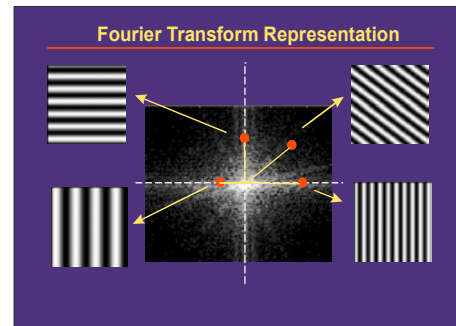


**Figure 25.** Various points in K-space (center) and their corresponding “stripe” functions in the image domain.

consider balls towards the centre of the array, the rotation rate of the balls decrease until we reach the centre ball where the magnetic field deviation is zero. Continuing further to the right, we see that the field is increasing

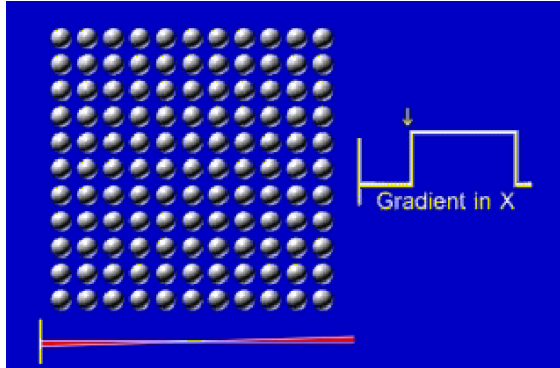


**Figure 27.** An array of spins just before the application of a  $G_x$  gradient.

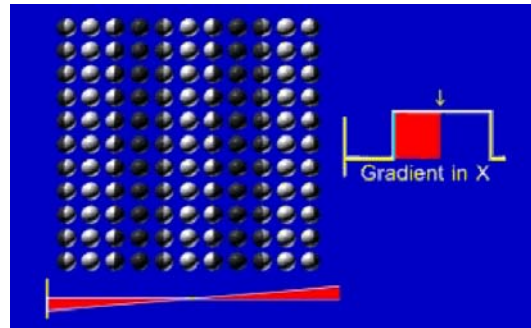


**Figure 28.** The application of a  $G_x$  gradient on the phase of the array of balls to create vertically oriented stripe patterns with increase in density with increasing  $G_x$  area (red).

gradually and results in a counter clockwise rotation rate of gradually increasing frequency. If we consider a later time (FIGURE 28) in the gradient evolution, we see that the balls are arranged to show varying degrees of black and white and a vertical stripe pattern emerges. The density of the stripe pattern (ie the spatial frequency), increases with the gradient evolution or the area under the gradient waveform (the red region of FIGURE 28). By orienting the gradient horizontally (along the X-axis), the stripe pattern is vertical. To create a horizontal stripe pattern, we apply the gradient along the Y-axis and see a progression of stripe density evolution with increasing gradient application as shown in FIGURE 29. Thus by application of a gradient in either the horizontal or vertical directions, we can generate stripes in the vertical and horizontal directions respectively. With increasing exposure to these gradients, the spatial frequency of the stripe pattern increases in proportion to the area under the gradient-time plot (shown red or green in FIGURES 28 and 29).

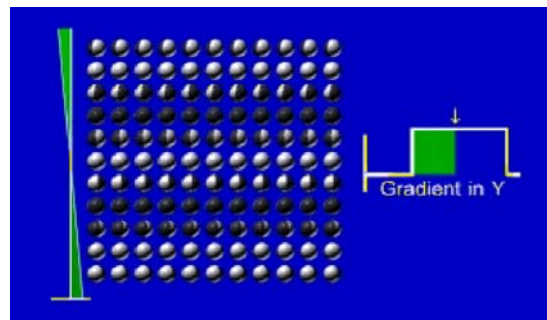


**Figure 29.** The application of a  $G_y$  gradient creates horizontally oriented stripe patterns.

### Stripe Patterns of Arbitrary Orientation and Spatial Frequency

In order to generate a stripe pattern in an arbitrary direction, we consider the use of two gradients in sequence. This is shown in FIGURE 30, where we show a plot of the gradient in  $G_y$  and  $G_x$  as a function of time. As shown, the amplitude of the  $G_y$  gradient waveform is incremented in steps (with fixed duration) after which a fixed  $G_x$  gradient waveform is applied. We also consider a plot where we trace out a trajectory which corresponds to the area of the gradient waveforms as they evolve. In this plot the horizontal axis is the area of the  $G_x$  gradient (red area) and the vertical axis is the area under the  $G_y$  gradient (green area). Recall that the spatial frequency of the stripe pattern increases with increasing exposure to a gradient and is represented by the area of the under the gradient waveform. Thus the area of the  $G_x$  gradient corresponds to the spatial frequency  $K_x$  while the area under the  $G_y$  gradient corresponds to the value of  $K_y$ . Thus, as we increment the  $G_y$  gradient amplitude, a point on this plot moves progressively along the  $K_y$  axis. After each  $G_y$  gradient application, the evolution of the  $G_x$  gradient causes that point to progress along

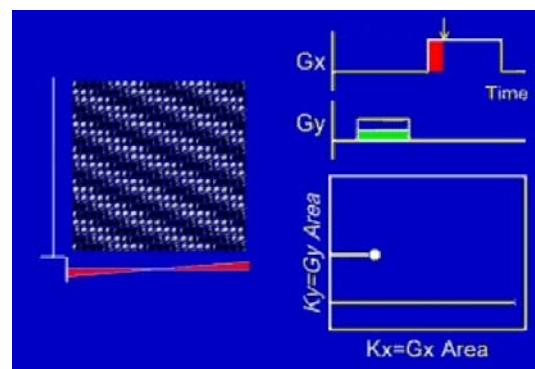


**Figure 30.** Creating stripe patterns in arbitrary directions with the sequential application of  $G_y$  and  $G_x$  gradients. A K-space plot traces out the area of the  $G_x$  and  $G_y$  gradient for the  $K_x$  and  $K_y$  locations respectively.

the  $K_x$  direction. Thus by combined application of the  $G_x$  and  $G_y$  gradients, we can move throughout all points in the  $K$ -space plot. To show that the combined application of  $G_x$  and  $G_y$  creates oblique strip patterns of varying spatial frequency, we consider the application of an intermediate choice of  $G_y$  followed by the  $G_x$  gradient in FIGURE 30 which illustrates one trajectory through  $K$ -space. However, if we considered all possible combinations of incremented  $G_y$  waveforms followed by the  $G_x$  gradient, we would have created all possible combinations of stripe orientation and spatial frequency for a Fourier representation of the object.

### Determining the $K$ -Space Amplitude of the Stripe Pattern

At this point in our discussion, we have shown how the application of gradients can create stripe patterns of varying orientation and spatial frequency. The only remaining issue to illustrate, is how the MR imaging system determines the correct amplitude for each spatial frequency needed to correctly encode the object. This is done by measuring the time dependent magnetization of the object during the application of the  $G_x$  gradient (FIGURE 31). Here, we represent the object as a transverse head image made up of our tiny magnetization spheres. During the application of the gradient, the spheres generate the stripe patterns that we have discussed above and generate an NMR signal which is induced in the RF coil. This signal is sampled periodically during the application of the  $G_x$  gradient to create a detected NMR signal. The amplitude of this signal corresponds to the desired  $K$ -space amplitude for each point in the  $K$ -space plot. After repeated applications of all the  $G_y$  and  $G_x$  gradients, the full  $K$ -space representation is complete.

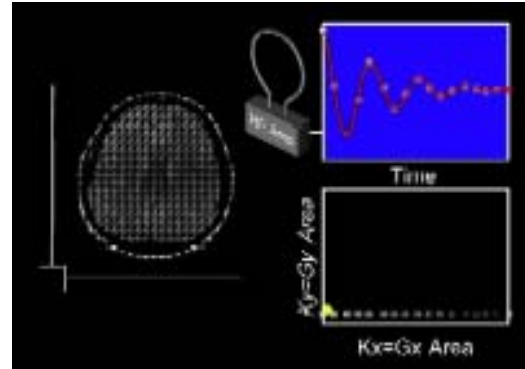


**Figure 31.** The signal detected during the  $G_x$  gradient becomes the weighting of the  $K$ -space data for each line in  $K$ -space.

### Final MRI Pulse Sequence

We can summarize what we have said about the  $K$ -space plot and now build a complete MRI pulse sequence as shown in FIGURE 32. During the RF pulse, a slice is selected in the presence of a  $G_z$  gradient. Then

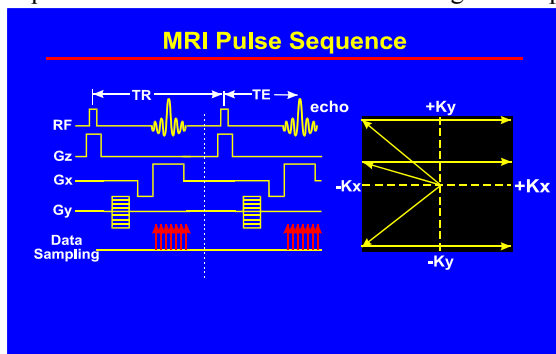


**Figure 32.** The final MR pulse sequence needed to scan throughout  $K$ -space showing the meaning of TR and TE to control image contrast.

an incremented  $G_y$  gradient is used to precede the  $G_x$  gradient waveform. The NMR signal or echo is “sampled” during the application of the  $G_x$  gradient. The sampled data is then applied to the corresponding trajectory in  $K$ -space to dictate the brightness of the  $K$ -space data. If  $N$  by  $N$  pixels in the  $x$  and  $y$  direction are needed in the final image, then we must sample the echo with  $N$  times for each of  $N$  incremented  $G_y$  gradient waveforms. This indicates that  $N$  separate echoes are needed in order to collect the  $N$  incremented  $G_y$  gradient applications. The timing between the successive  $G_y$  gradients is TR seconds and is the parameter used to control the T1 weighting of the image as discussed above. Similarly, the time between the selective excitation pulse and the peak of the echo formation is the TE time and is used to determine the amount of T2\* weighting in an image.

### Conclusions and Final Comments

In this summary of the ISMRM lecture, we have attempted to summarize the physics of NMR and the dynamics of proton ‘spin gymnastics’ that work together to make MRI possible. We see that the traditional means of describing how frequency and phase encoding have not been mentioned in this presentation. Rather, we describe how the application of  $G_x$  and  $G_y$  gradients in tandem can provide all the data needed to provide a Fourier representation of the object. While the intuitively simple notion of frequency encoding is straight forward, it does not translate smoothly into a correspondingly simple interpretation of phase encoding. As such, the perception is often held that frequency and phase encoding are different concepts which can be misleading. However, as presented here, it should be clear that frequency and phase encoding are indeed slightly different ways of achieving the same thing, that is to generate the stripe patterns needed to collect the  $K$ -space data of the object.

## Further Reading

A number of excellent texts have been written on the subject of MRI. I would recommend the following.

- 1) Magnetic Resonance Imaging; eds DD Stark and WG Bradley. Mosby Year Book. 2<sup>nd</sup> edition. 1992. A thorough but slightly dated text.
- 2) Magnetic Resonance Imaging. Physical Principles and Sequence Design. EM Haacke, RW Brown, MR Thompson R Venkatesan. Wiley-Liss. 1999. A more complete and somewhat theoretically oriented text. An excellent text for graduate students interested in MRI.
- 3) Principles of Nuclear Magnetic Resonance Microscopy. Paul T Callaghan. Oxford Science Publications, 1991. Again a slightly older text, but thorough with an interested emphasis on high resolution imaging.

Furthermore a number of very introductory online tutorials on MRI are available. I would recommend the following:

- 1) [http://www.hull.ac.uk/mri/lectures/Gpl%20web%20page/gpl\\_page.html](http://www.hull.ac.uk/mri/lectures/Gpl%20web%20page/gpl_page.html)
- 2) <http://www.mritutor.org/mritutor/>
- 3) <http://www.cis.rit.edu/htbooks/mri/>